Research Square

Preprints are preliminary reports that have not undergone peer review.
They should not be considered conclusive, used to inform clinical practice,
or referenced by the media as validated information.

Dynamic Changes in Lakes within the Selin Co Basin and Potential Drivers in Tibet

Wenhui Liu (liuwenhui222@126.com)
Qinghai University https://orcid.org/0000-0002-1646-8201
Hairui Liu
Qinghai University
Changwei Xie
Chinese Academy of Sciences
Guangyue Liu
Chinese Academy of Sciences
Wu Wang
Chinese Academy of Sciences
Qi Zhang
Qinghai University
Qinhao Zhang
Qinghai University

Research Article

Keywords: Lake changes, Driving factor, Glacier melting, Permafrost degradation, Selin Co basin

Posted Date: April 27th, 2021

DOI: https://doi.org/10.21203/rs.3.rs-379356/v1

License: This work is licensed under a Creative Commons Attribution 4.0 International License. Read Full License

Abstract

Prevailing lake changes on the Qinghai-Tibetan Plateau (QTP) have occurred. Selin Co, a representative saline lake in the central region of the QTP, has experienced significant expansion, but the main cause for its dramatic expansion is still under debate. Based on Landsat images, meteorological data, and glacier and permafrost data, the dynamic changes in Selin Co and its surrounding small lakes were systematically discussed, and the driving factors behind these changes were further explored. The results suggest that from 1988–2017, the areas of Bange Co and Cuoe Lake showed slow, overall increasing trends at rates of 0.28 km^2/yr and 0.11 km^2/yr, respectively, and they exhibited upward trends before 2005 but downward trends afterward. The area of Selin Co substantially increased by 685.8 km^2 with a growth rate of 30.39 km^2/yr, with a slow increase of 27.11 km^2 during the period from 1988–1997, a rapid increase of 510.53 km^2 from 1997–2005 and an increase of 148.16 km^2 from 2005–2017. Accordingly, the lake level and water volume of Bange Co slightly increased by 1.64 m and 0.088 km^3, respectively, whereas those of Selin Co significantly rose by 8.138 m and 17.47 km^3, respectively. The changes in the areas of Bange Co and Cuoe Lake were mostly related to annual precipitation (AP). Enhanced glacial meltwater owing to rising, with a rapid reduction of 165.1 km^2 (39%) in the glacier area in the basin between 1980 and 2010, predominantly drove the dramatic expansion of Selin Co, followed by accelerated permafrost degradation, with significant increases in the active layer thickness (ALT) (7.44 cm/yr) and soil temperatures at a 15-m depth (0.0346°C/yr).

1 Introduction

The Qinghai-Tibetan Plateau (QTP) contains 1236 lakes (> 1 km^2) with an area of ~ 41,800 km^2, which accounts for 39.2% and 51.4% of total lake number and area in China (Ma et al. 2011; Zhang et al. 2014). Lakes on the QTP have experienced substantial changes in surface area, water level and water volume; specifically, most lakes have experienced the significant lake expansion since 2000 (Liu et al. 2009; Lei et al. 2013; Lei et al. 2014; Li et al. 2014; Song et al. 2014; Yang et al. 2017A; Yang et al. 2017B; Zhang et al. 2017a, b; Zhang et al. 2018; Yao et al. 2018; Liu et al. 2020a; Zhang et al. 2021). Among the expanding lakes, the Selin Co lake has had the largest increase. Its area (2,016.95 km^2) exceeded the area of Nam Co (1,984.83 km^2) in 2001, and it has become the largest endorheic lake in Tibet. The growth of Selin Co has been discussed by many quantitative and qualitative studies (Bian et al. 2010; La et al. 2011; Zhang et al. 2011; Meng et al. 2012a; Du et al. 2014; Zhou et al. 2015; Hao et al. 2016; Deji et al. 2018), but the main cause for its dramatic expansion is still debated. A consensus illustrated that increasing glacier meltwater has played a dominant role in the expansion of Selin Co (Bian et al. 2010; La et al. 2011; Meng et al. 2012a; Du et al. 2014; Hao et al. 2016; Deji et al. 2018), while Liu et al. (2019) found that the contribution of glacier mass changes to lake level rise in the Selin Co basin is only 5.52%, and glacier melting is not the main driving force of the lake level rise. Zhang et al. (2011) demonstrated that both participation runoff increases and evaporation decreases have led to the Selin Co expansion. Lei et al. (2013) suggested that although decreased lake evaporation and glacier mass loss contribute to the growth of the lake to a certain extent, the overall lake growth is mainly owing to the significant increase in precipitation. Zhou et al. (2015) found that the main contribution of lake inflows to the water storage change of Selin Co was approximately 49.5%.

As rising air temperatures on the QTP, permafrost has been degraded seriously (Wu and Zhang 2010; Wu et al. 2010; Li et al. 2012; Xie et al. 2012; Xie et al. 2015; Liu et a. 2016; Zou et al. 2017; Cheng et al. 2019; Zhao et al. 2020; Sun et al. 2020). Under the circumstances of permafrost degradation, the melting of ground ice and the release of soil water content in permafrost, as well as increasing aquifer thicknesses and surface water infiltration amounts arising from increasing active layer thicknesses (ALT), are expected to impact groundwater dynamics and enhance the hydraulic exchange between surface water and groundwater and further change the recharge, discharge and movement patterns of surface water and groundwater (Walvoord et al. 2012; Kurylyk et al. 2014; Walvoord and Kurylyk 2016; Liao and Zhuang 2017). The hydrological effects of permafrost degradation on rivers and lakes have been detected in basins in the northwestern China (Niu et al. 2011), Qilian Mountains (Li et al. 2014; Li et al. 2016; Wang et al. 2017; Wang et al. 2018; Gui et al. 2019) and QTP subbasins (Song et al. 2020; Ji 2020). Recent studies have even quantitatively indicated that meltwater from permafrost degradation was responsible for 20%~21% of the outlet runoff in the Hulugou River and Shiyang River basins (Li et al. 2014; Li et al. 2016) and for 24%±2.4% of the mean runoff in the Gulang River basin (Gui et al. 2019). The melting of ground ice at shallow depths below the permafrost table in an endorheic basin on the QTP was found to account for 21.2% of the increase in lake volume from 2000 to 2016 (Liu et al. 2020b).

For the Selin Co basin, because of the lack of permafrost information, the effect of permafrost thawing on lake change has rarely been considered in previous studies. In reality, continuous permafrost is widely distributed in the Selin Co catchment with a large amount of underground ice content in permafrost regions. It is likely that permafrost degradation plays a significant role in influencing the hydrological regime and water resources in the catchment and eventually results in enhanced lake growth. In addition, most of the above studies focused on the area and lake height variations in a single lake (Selin Co), while comparative studies from the perspective of lake bodies lumped together under similar climate conditions are rarely involved. This is insufficient to accurately analyze the influence of local climate conditions on lake change, as well as the influences of glaciers and permafrost. Therefore, it is necessary to analyze the relationship between the changing trends of lake group areas and influencing factors. In this paper, based on multi-remote sensing images, meteorological data, glacier data and permafrost monitoring data, the dynamic variations in Selin Co and its surrounding lakes during the period from 1988–2017 were discussed, and the driving factor behind their changes was further explored with a comprehensive consideration of various factors. The main objective of this study is to improve the understanding of the significant responses of lake changes to climate conditions at the basin scale over the QTP.

2 Data And Methods

2.1 Study area

Bange Co, Cuoe Lake and Selin Co are enclosed salt lakes in the central QTP; these lakes are located in Nagqu Prefecture, Tibet (Fig. 1). The study area covering Selin Co-Bange Co has a characteristic semiarid climate, with a mean annual air temperature (MAAT) of 0.78°C, annual precipitation (AP) of 315 mm, annual evaporation (AE) of 2,080 mm, wind speed of 3.9 m/s and relative humidity of 42%, as well as an average annual sunshine duration of 2,950 hours (Zhang et al. 2011). Precipitation mainly occurs from May to September. The Selin Co lake (31°32.7'N ~ 32°7.8'N, 88°31.7'E ~ 89°21.7'E) is distributed at the junction of Shenzha, Bango and Nima counties. It had an average surface elevation of 4,545.7 m a.s.l. during the period from 2000–2015 and an area of 2,059.5 km^2 during the period from 1988–2017 (from this study), with a maximum length of 80 km and width of 66 km (Zhang et al. 2013). The Selin Co catchment has an area of 45,530 km^2 with the Tanglha and Nyamqentanglha Mountains to the south. Several major rivers flow into Selin Co from different locations, including the Zajia Zangbo River from the north shore of the lake, Boqu Zangbo River from the east shore of the lake and Zagen Zangbo River from the west shore of the lake; among these rivers, Zajia Zangbo River is the longest river on the QTP with a length of 409 km (Bian et al. 2010; Du et al. 2014). The lake is mainly supplied by Geladandong Glacier, which is located in the upstream region of the basin and serves as a major water source for the lake (Zhang et al. 2011). There are many small lakes over the Selin Co basin, among which Cuoe Lake is nearest to Selin Co and has an area of 271.85 km^2. Its main supply originates from the Daergawa Zangbo River and Xiagang Zangbo River, which flow from the southeast into the lake. Bange Co (31°47.21'N, 89°30.34'E) is located in Bango County. The average surface area was 126.37 km^2 during the period from 1988–2017, and the surface elevation was 4,521.22 m during the period from 1959–2003 (from this study). As shown in Fig. 1, it consists of Bange I, II and III. Bange I is a seasonal lake that is filled only by water in the rainy season and covers an area of 5.4 km^2. Since 1983, due to the rising water level, Bange II and Bange III have merged into one larger lake (named Bange Co) with an area of 130 km^2 and depth of approximately 1.1 m (Zhao et al. 2006). The lake is supplied by snow meltwater via the Qiaga Zangbo River. A small wetland with an area of 35.89 km^2 is distributed in the catchment, covering an area of 2,479.77 km^2.

2.2 Remote sensing

Landsat data (http://glovis.usgs.gov) provided more available information for delineating the lakes. Landsat Thematic Mapper (TM), Enhanced Thematic Mapper Plus (ETM+) and Operational Land Imager (OLI) images free of or with small fractions of cloud coverage (< 10%) were chosen to extract the lake surface areas and create a continuous time series of areal changes between 1988 and 2017. All of the images were acquired in October because lake areas in this month are relatively stable (Zhang et al. 2017c). Thirty scenes were used to delineate lakes between 1988 and 2017, and 36 scenes (one scene for each month) were acquired to determine the seasonal scale of the lake areas during the period from 2015–2017. The lake boundaries were extracted from the false color compositions (bands 5, 4, and 3 for Landsat TM/ETM + and bands 7, 6 and 5 for Landsat OLI as red, green, and blue, respectively) of raw Landsat images for each lake in ENVI 5.3. Then, visual examinations and manual editing of lake boundaries were conducted to delineate lakes in ARCGIS 10.2. All the map and image data were projected into the UTM coordinate system Zone 45 using the WGS-84 geodetic datum. The accuracy of manual digitization was controlled within one pixel.

Lake level changes over the QTP are poorly understood due to remoteness, high altitude, thin atmosphere, and harsh weather conditions in the region. Satellite altimetry can serve as a powerful and complementary tool for hydrologic monitoring and studies. The water level changes of Selin Co were studied using the Globe Lake Level Change Dataset (http://www.geodoi.ac.cn/webcn/doi.aspx?id=990), which was produced by Liao et al. (2018). This dataset was compiled through lake boundary delineations, water level calculations, outlier removal, Gaussian filtering, and elevation system conversions based on multialtimeter data (Cryosat-2, Jason-2 and ENVISAT/RA-2). It contains lake level during 2002–2017 for 87 lakes in High Mountain Asia, and the error between the water levels of lakes from this dataset and from the Hydroweb water level products was less than 1 m.

2.3 Meteorological data

The air temperature, precipitation and evaporation data from the Bange (90.01°E, 31.23°N, 4,700 m a.s.l.) and Shenzha (88.38°E, 30.57°N, 4,672 m a.s.l.) meteorological observation stations provided by the National Meteorological Information Center (NMIC) of the China Meteorological Administration (CMA) (http://cdc.cma.gov.cn) were used to analyze the correlations between climatic factors and lake changes. Air temperature data at the Tanggula meteorological observation station (91.93°E, 33.06°N, 5,100 m a.s.l.) was provided by the Cryosphere Research Station on the Qinghai-Tibet Plateau, Chinese Academy of Sciences; this data was used to indicate the temperature conditions in glacier and permafrost regions in the area upstream of the Selin Co basin.

2.4 Glacier and permafrost data

The First and Second Glacier Inventory of China (http://westdc.westgis.ac.cn) and the latest glacier dataset from Ye et al. (2017) were used to extract glacier coverage in the basin. Permafrost monitoring data were provided by the Cryosphere Research Station on the Qinghai-Tibet Plateau, Chinese Academy of Sciences. Soil temperatures at the active layer observation site (QT04) were monitored using 105T thermistor sensors with an accuracy of 0.1°C. Soil temperatures at the borehole site (QTB15) were monitored using thermistor sensors, which were made at the Chinese State Key Laboratory of Frozen Soil Engineering at Lanzhou and exhibited excellent sensitivity (± 0.01°C) in laboratory tests. These thermistor sensors were deployed at different intervals at different depths (Table 1). The instruments were attached to a CR1000 data logger (Campbell Scientific). Soil temperatures for the active layer were collected once every 30 min, and soil temperatures for the boreholes were automatically recorded 12 times per day at 2-hour intervals. The ALT was determined by measuring the maximum depth of the 0°C isotherm, as observed from the soil temperature profiles. Soil temperatures at a 15-m depth recorded from the borehole sites were used to describe permafrost temperatures in this study, because the zero-amplitude depths ranged from 10 to 15 m on the QTP. Permafrost temperatures at a 15-m depth were generally within − 2°C from the freezing point except in a few mountainous areas, which avoids effect of seasonal temperature variation (Wu et al. 2010). The ground ice content in the basin was extracted from the distribution of the ground ice content

over the QTP, which was calculated by the following formula: $Gi = \int \rho_d(Z)\theta(Z)dZDs$, where *Gi* is the ground ice content (kg), is the bulk density of the soil ($kg \cdot m^{-3}$), is the gravimetric water content of the soil (%), *Z* is the permafrost thickness (m) and *S* is the permafrost area (m^2).

Table 1
Geographic information of the active layer observation site and borehole site.

Station number	Lon (°E)	Lat (°N)	Altitude (m)	Underlying surface type	Thermistor sensors depth (cm/m)	ALT (m)	MAGT (°C)	DZAA (m)
QT04	91.02	32.97	5,100	Degraded alpine frost meadow	2cm,5cm,10cm,20cm, 50cm,70cm,90cm,105cm, 140cm,175cm,210cm, 245cm,280cm,300cm	3.6	-	-
QTB15	91.89	33.09	4,960	Alpine frost meadow	0.5 ~ 5m: 0.5-m interval 5 ~ 10m: 1-m interval 10 ~ 20m: 2-m interval > 20m: 5-m interval	4.0	-1.2	17

Note: MAGT is the mean annual ground temperature; DZAA is the depth of the zero annual amplitude of the ground temperature of permafrost.

3 Results

3.1 Area changes

3.1.1 Annual changes

The areas of Bange Co, Cuoe Lake and Selin Co showed overall increasing trends between 1988 and 2017; the areas increased by 2.56 km^2, 2.83 km^2 and 685.80 km^2 at rates of 0.67 km^2/yr, 0.11 km^2/yr and 30.39 km^2/yr, respectively (Fig. 2). Both Bange Co and Cuoe Lake experienced similar change trends; the lake areas presented upward trends before 2005 (decreasing during the period from 1988–1995 and increasing during the period from 1995–2005) but downward trends afterward. The area of Bange Co increased from 114.60 km^2 in 1988 to 145.40 km^2 in 2005, showing an increase of 30.80 km^2 at a rate of 1.27 km^2/yr, but its area decreased to 117.17 km^2 in 2017 with a decrease of 28.24 km^2 at a rate of 1.98 km^2/yr after 2005. The area of Cuoe Lake first slightly increased by 3.90 km^2 at a rate of 0.40 km^2/yr, then decreased by 1.07 km^2 at a rate of 0.19 km^2/yr. Specifically, during the period from 1988–2005, the areas of Bange Co and Cuoe Lake decreased by 10.82 km^2 and 3.43 km^2, respectively, then increased by 41.62 km^2 and 7.34 km^2, respectively (Fig. 2a). Unlike the former two lakes, the area of Selin Co exhibited three increasing stages; it slowly increased by 27.11 km^2 at a rate of 2.05 km^2/yr from 1988–1997, quickly increased by 510.53 km^2 at a rate of 64.55 km^2/yr from 1997–2005 and slightly increased by 148.16 km^2 at a rate of 13.25 km^2/yr from 2005–2017 (Fig. 2b). The area changes of Selin Co agreed well with previous results from Meng et al. (2012a). Selin Co also experienced a slight increase, accelerated growth, and a relatively slow increase during the period from 1976–2009, with a total increase of 656.64 km^2 (39.4%).

Lake changes during the period also occurred simultaneously in sizes. The shapes of the three lakes changed accordingly, especially dramatic changes in Selin Co (Fig. 3). The shape of Bange Co changed slightly; these changes occurred in the shallow areas east of Bange II. Cuoe Lake expanded southward continuously. There was an opening in the west that was closed in some years so that a large rock island in the west of the lake was inundated. Mainly, a significant change in the shape of Selin Co was observed; the lake expanded rapidly northward, southward and southeast-southward, and marked expansion occurred along the lake shoreline in the southeast direction. The maximum expansion distance was approximately 146.7 m in the northwest direction. Notably, Yagedong Co rapidly enlarged, and it connected with the main body of Selin Co in 2004. Selin Co also expanded northward in 2005. Both these factors resulted in the sharp expansion of Selin Co during the period from 2004–2005.

3.1.2 Seasonal changes

As shown in Fig. 4, the areas of Bange Co and Selin Co displayed obvious seasonal oscillations. When spring began, the areas rapidly increased and experienced peaks in May, then continuously increased and reached annual maximums in summer, then finally sharply decreased after autumn. The area of Bange Co experienced peak values in March, May and July, and the area of Selin Co peaked in January, May and September. The area experienced minimum values in April for Bange Co and in March for Selin Co. The lake areas were generally stable when the lakes froze in winter. The peaks and valleys observed in winter were due to large snow coverage, which caused overdelineations of the lake boundaries. This commonly occurred for Bamu Co and Zonag Lake on the QTP, with valleys observed in February and March, respectively (Bhasang et al. 2012; Liu et al. 2019).

3.2 Changes in the lake levels and water volumes

Despite the lack of lake level data in some years, water level elevation data of Bange Co reconstructed from the lake shorelines at different dates from previous studies (Zhao et al. 2006; Zhao et al. 2011) revealed that the lake level has risen slightly since 1959 with an increase of 1.64 m; the water surface elevations were 4520.76 m in 1959 and 4522.5 m in 2010 (Fig. 5a). Due to data discontinuities since 2003, the variation in the lake level during the period

from 1959–2003 was analyzed significantly. From 1959 to 2003, the lake level slowly fell by 0.25 m from 1959–1973, slightly rose by 1.75 m from 1973–2000 and then fell by 0.72 m from 2000 to 2003. Between 2000 and 2015, the lake level of Selin Co also displayed an upward trend, with a rise of 8.138 m at a rate of 0.48 m/yr. It markedly rose by 6.92 m during the period from 2000–2005 but relatively slowly rose by 1.21 m from 2005–2015 (Fig. 5b). There was a marked correspondence between lake area and lake level in which a rapid increase occurred before 2005; the area of Selin Co significantly increased by 357.65 km^2 at a rate of 70.38 km^2/yr between 2000 and 2005, compared to an increase of 156.68 km^2 at a rate of 16.69 km^2/yr during the period from 2005 to 2015. Specifically, between 2003 and 2009, Selin Co experienced a relatively fast water-level rise of 3.80 m (0.59 m/yr), which was consistent with the increases in the water level of Selin Co estimated by numerous studies due to the use of available ICESat data since 2003, as well as the water level fluctuations of other alpine lakes. Selin Co was reported to exhibit significant water-level rises of 4.79 m (0.625 m/yr) (Song et al. 2013) and 4.37 m (0.69 m/yr) (Zhang et al. 2013) during the period from 2003–2009.

Based on lake area and lake surface elevation data, the lake volume was calculated as follows: $\nabla V = \frac{1}{3}(H_2 - H_1) \times (A_1 + A_2 + \sqrt{A_1 \times A_2})$, where ∇V is the lake volume change from area (A1) and lake surface elevation (H1) to area (A2) and lake surface elevation (H2) (Zhang et al. 2013). From 1988 to 2010, the lake volume of Bange Co slightly increased by 0.088 km^3, during which increases of 0.025 km^3 from 1988 to 2003 and of 0.065 km^3 from 2003 to 2010 were detected (Table 2). During the period from 2000–2015, as the lake water level increased by 8.13 m and the lake area increased by 514.33 km^2, the lake water volume of Selin Co dramatically increased by 17.47 km^3. Likewise, the trend in the lake water volume before and after 2005 was similar and highly consistent with those of the lake area and lake level; the water volume substantially increased by 14.63 km^3 during the period from 2000–2005 but slightly increased by 2.84 km^3 from 2005–2015. This was well explained by the significant shape change described above; Yagedong Co merged into the body of Selin Co in 2004, and the lake rapidly expanded northward from 2014–2015.

Table 2
Changes in the lake volumes of Bange Co and Selin Co.

Lake	Period	Elevation change (m)	Area change (km^2)	Volume change (km^3)
Bange Co	1988–2010	0.69	8.55	0.088
	1988–2003	0.2	13.35	0.025
	2003–2010	0.49	-4.79	0.065
Selin Co	2000–2015	8.13	514.33	17.47
	2000–2005	6.92	357.65	14.63
	2005–2015	1.21	156.68	2.84

3.3 Influential factors

3.3.1 Climate factors

The average annual precipitation (AP), mean annual air temperature (MAAT), and annual evaporation (AE) during the period from 1988–2017 recorded at the Bange Co and Shenzha meteorological stations were 345.5 mm and 345.1 mm, 0.003°C and 0.63°C, and 1,926.2 mm and 1,914.2 mm, respectively. Both the AP and MAAT at the two stations displayed overall increasing trends; the AP increased at rates of 1.38 mm/yr and 2.95 mm/yr, and the MAAT rose at rates of 0.05°C/yr and 0.04°C/yr at the Bange Co and Shenzha stations, respectively (Fig. 6a); however, during the same period, AE declined at rates of 10.68 mm/yr and 16.12 mm/yr, respectively (Fig. 6b), which was in accordance with the quantitative estimation that a nonsignificant decrease in actual evaporation of 4.17 mm/yr was observed for the lake area of Selin Co (Zhou et al. 2016). This climatic characteristic is consistent with the observations that the climate in most regions on the QTP experienced rapid warming-wetting in the late 20th century and early 21st century (Yang et al.2011; Li et al. 2018). It is also obvious that the variation trends in AP, MAAT and AE were generally similar for the two meteorological stations, with consistent peak and valley values, especially maximum values in 2009 and minimum values in 1997, which commonly represent local climatic conditions within the Selin Co basin.

The increasing trends in AP and MAAT exhibited three stages. The AP sharply decreased from 1988–1995, gradually increased from 1995 to 2005 and then slowly decreased (Fig. 7a). The MAAT gradually fell from 1988 to 1997, rapidly rose from 1997 to 2007 and then slowly rose (Fig. 7b). A significant decreasing trend in AE was observed from 1988 to 2017, which also displayed three stages (Fig. 7c). AE gradually declined from 1988 to 1997 but increased from 1997–2007; these variations were attributed to the decreasing and increasing MAAT, respectively. After 2007, AE sharply declined, and the decrease in wind speed may have been responsible for these changes. The area changes of Bange Co and Cuoe Lake corresponded well to the variations in the AP. The lake areas decreased slightly from 1988–1995, which agreed with the decrease in the AP. The lake areas continuously increased from 1995 to 2005 with increasing AP. After 2005, the lake areas decreased with increasing AP. This result suggested that the changes in the areas of Bange Co and Cuoe Lake were closely associated with the AP, and precipitation was the most critical influencing factor. However, the area change of Selin Co coincided with the increasing MAAT. The area of Selin Co slowly increased from 1988 to 1997 with a slight increase in the MAAT, quickly increased from 1997 to 2005 due to a rapid increase in the MAAT and slowly increased from 2005 to 2017 with a slight increase in the MAAT. This indicates that the rapid expansion of Selin Co had a close relationship with the continuous increase in the MAAT, as the MAAT has important impacts on glacier ablation processes and permafrost thawing. The

area changes of the three lakes were inconsistently correlated with AE; the areas decreased slightly from 1988–1995 as AE declined, continuously increased from 1995 to 2005 with increasing AE and then decreased in spite of the declining AE.

3.3.2 Glacier contribution

Bange Co and Cuoe Lake are nonglacier-fed lakes, and their water budgets mainly depend on precipitation and evaporation. As mentioned above, precipitation was the main driver behind their observed changes. Selin Co is a glacier-fed lake with high glacier coverage in its basin. There were 297 glaciers with a total area of 423.09 km^2 in 1980, accounting for approximately 1% of the basin area. Lakes supplied by many glaciers within their catchments may be more affected by increasing glacial meltwater than by precipitation (Zhang et al. 2011). As the MAAT recorded at Tanggula meteorological station increased at a rate of 0.03°C/yr between 2005 and 2015 (Fig. 8a), glaciers in the Selin Co catchment considerably retreated. The statistical results showed that from 1980 to 2010, the total glacier area decreased by 165.1 km^2 (39%); during this period, it decreased by 25.9 km^2 (6%) from 1980 to 2001 and by 139.1 km^2 (35%) from 2001 to 2010 (Fig. 8b). For Selin Co, a highly glacierized lake in a catchment on the QTP, such considerable glacier ablation generated a large amount of surface runoff from glacier meltwater, which contributed to the extension of Selin Co. Strong positive relationships between lake area change and glacier area change were observed for most large lakes on the QTP (Liu et al. 2020). In addition, a more rapid decline in glacier area was observed during the period from 2001–2010, corresponding well to a much larger rise since 2000. Meng et al. (2012a) derived lake water level variations from topographic maps and GPS measurements and found that the water level of Selin Co increased by 8.2 m between 2000 and 2010 at a rate of 0.82 m/yr compared to a rise of 4.3 m between 1976 and 2000 at a rate of 0.18 m/yr. This further suggested that increasing meltwater supply from glaciers is the dominant factor behind the rapid expansion of Selin Co.

The lake supply coefficient was defined as the ratio of the basin area to the lake area, as follows: ($A_C=A_B/A_L=(E_L-P_L)/(rP_B)+1$), where A_C is the lake supply coefficient; A_B and A_L are the basin area and lake area, respectively; E_L and P_L are the lake surface evaporation and precipitation, respectively; P_B is the precipitation in the basin; and r is the runoff coefficient. For an endorheic lake, P_L is equal to P_B, which means that the lake supply coefficient (A_C) mainly depends on the lake surface evaporation (E_L) and runoff coefficient (r) (Li et al. 2011). For glacier-fed lakes, positive correlations between water-level rising rates and supply coefficients were also reported for lakes in the Pamir and Tienshan Mountains and on the QTP (Li et al. 2011; Song et al. 2014). Due to the large lake watershed area, Selin Co has a large supply coefficient of 18.9 based on a basin area of 45,530 km^2 and a lake area of 2,405.65 km^2 as measured in 2017; this large coefficient also accelerated lake growth to a certain extent. In comparison with Nam Co, which has a supply coefficient of 5.36 (Song et al. 2014), although the two lakes have similar glacial meltwater supplies, the much larger supply coefficient of Selin Co may partly account for its more rapid growth rates than those of Nam Co.

3.3.3 Permafrost degradation

The largest permafrost degradation on the QTP has occurred in the marginal zones of the permafrost region (Pang et al. 2011; Qin et al. 2017), and permafrost over Selin Co was distributed only in its southern marginal zones. The island of permafrost was distributed in the southeastern basin with an area of 76.38 km^2, accounting for only 3% of the whole Bange Co catchment. The ground ice content was only 0.39 km^3. For Selin Co, continuous permafrost was distributed in the northeastern basin with permafrost coverage of 1.3×10^4 km^2, and an island of permafrost was distributed in the southern basin with a small area. The ground ice content over the basin was 148.4 km^3 with a range of 2.0 ~ 85.2×10^6 m^3 (Fig. 9a). As evidence of significant permafrost degradation, both the ALT at the QT04 observation site and the ground temperature of permafrost at a 15-m depth at the QTB15 borehole site drilled upstream of the Selin Co basin experienced increasing tendencies. The ALT increased by 58.7 cm at a rate of 7.44 cm/yr from 2006–2019, and the soil temperatures at a 15-m depth rose at a rate of 0.0346°C/yr from 2005–2017 (Fig. 9b). The increase in the ALT here was much larger than that of the ALT (1.29 cm/yr) on the whole QTP (Xu et al. 2017), and an increase of 1.96 cm/yr was determined for the ALT along the Qinghai-Tibet Highway from 1981–2017 (Liu et al. 2020b). This result suggested that accelerated permafrost degradation around Selin Co occurred.

As permafrost degradation occurred, a large amount of ground ice content in the catchment melted; this melt was not only more likely to provide more water resources but also increased aquifer activation to enhance hydrological processes in the basin and further supply rivers and lakes, given the rise to a marked expansion of Selin Co. Meltwater directly influenced the groundwater recharge and water levels of Selin Co or increased the amount of groundwater discharge as surface drainage. Some of the meltwater even directly drained to become surface runoff and supplied Selin Co. Moreover, the presence of ice-rich permafrost in the Selin Co basin served as a barrier layer due to its low hydraulic conductivity and permeability (Yang et al. 2003; Woo et al. 2008; Wang et al. 2009). Ice-rich permafrost impeded liquid water infiltration and the interaction between surface water and groundwater, which finally resulted in a large amount of direct surface runoff due to both rain and snow-glacier melting due to the lack of a water storage buffer effect.

As shown in Table 3, precipitation from May-September mainly accounted for 93% of the annual precipitation in the study site. Both precipitation and the air temperature increased from April, reached maximum values in July, and decreased after July. Evaporation showed an obvious increase from January to April and then decreased, but it continued to increase after September and appeared to peak in October. Large areas of Bange Co and Cuoe Lake observed from May-August were mainly attributed to the most significant increases in precipitation. For Selin Co, glacier ablation runoff mainly occurred from July to September due to rising temperatures (Zhang et al. 2009). According to thawing and freezing processes of the active layer of permafrost near the Tanggula region, the active layer begins to thaw downwards from the ground surface at the end of April, and the thawing process reaches its maximum depth in late autumn (Zhao et al. 2000; Hu et al. 2014). Glacial meltwater and ground ice meltwater significantly participate in mountainous discharge in glacial regions, and this discharge is greater than precipitation in this basin (Zhang et al. 1997). Therefore, glacier melting and permafrost thawing with high air temperatures during the period from June-August can account for the large area of Selin Co observed during the period from August-November well, with a corresponding response lag. At the seasonal time scale, the relationship between lake group areas and influencing factors further confirmed that changes in the areas of Bange Co and Cuoe Lake were mainly related to increasing precipitation, and glacial and permafrost meltwater were significant factors influencing Selin Co growth.

Table 3
The statistics of monthly lake areas and meteorological elements from 2015–2017.

Climate factors	Jan	Feb	Mar	Apr	May	Jun	Jul	Aug	Sep	Oct	Nov	Dec
Precipitation (mm)	3.93	0.2	5.07	7.66	32.1	73.1	95.96	92.56	37.83	5.2	0.2	0.16
Percent (%)	1.11	0.05	1.43	2.16	9.06	20.64	27.10	26.14	10.68	1.46	0.05	0.04
Air temperature (°C)	-11.19	-6.27	-3.60	0.12	3.71	8.03	9.73	9.30	7.56	1.74	-3.40	-5.86
Evaporation (mm)	81.86	117.93	144	173.4	166.8	130.76	141.1	124.76	120.96	175.5	129.6	127.66
Percent (%)	5.00	7.21	8.81	10.60	10.20	8.00	8.63	7.63	7.40	10.73	7.92	7.81
Bange Co area (km^2)	111.1	111.5	115.1	108.9	116.4	116.9	117.9	117.8	115.5	113.0	112.0	108.6
Selin Co area (km^2)	2400.53	2400.40	2400.39	2400.53	2400.70	2400.73	2400.82	2400.97	2401.00	2400.96	2400.89	2400.75

4 Discussion

4.1 Hydraulic connection

Due to the strong summer monsoon-driven climate with temperatures 2 to 4°C higher and precipitation 40% to > 100% higher than the current values (Shi et al.1999; Shi et al. 2001), lakes on the QTP appeared to be in the “pan-lake stage” in the period of 40 ~ 25 ka B.P. During this time, the QTP was covered by large interconnected pan-lake systems with a total area of ~ 360,000 km^2 and a total volume of lake water > 530 million km^3, which were approximately 38 times larger than those of modern lakes (Zheng et al. 2006; Li 2000). Accordingly, there was an east-Qiangtang ancient lake with a surface elevation of 4630 m, which consisted of Selin Co, Nam Co, Beng Co, Yagedong Co, Bamu Co lakes, etc., that were all connected to each other (Zhu et al. 2001; Zhao et al. 2002; Zhu et al. 2003; Zhao et al. 2005; Zhao et al. 2011; Meng et al. 2012b; Zhao et al. 2018). After the greatest lake period, because of the reduced lake level arising from the rapid uplift of the QTP and the cold climate, the great lake contracted and fell apart, so Bange Co, Cuoe Lake, Wuru Co and Yagedong Co were separated from Selin Co as independent lakes during the late Late Pleistocene, when the QTP gradually evolved into its present appearance (Lv et al. 2003; Meng et al. 2012b; Zhao et al. 2018). Therefore, a significant viewpoint of the hydraulic connection between Selin Co and its surrounding lakes has been illustrated by many studies but is under debate.

Bange Co, an isolated lake from the eastern part of Selin Co (Fig. 10), was connected with Selin Co by a sandy spit that consisted of sandy sediments with high permeability. Some authors have stated that a strong hydraulic connection despite a straight-line distance of approximately 8 km was the main cause of the dynamic change in Bange Co as the Selin Co lake level increased (Zhao et al. 2006). However, Wu et al. (2009) denied this stable hydraulic connection of Selin Co, stating that the water level of Bange Co should be basically stable rather than showing such large fluctuations (decreasing during 1988–1995, increasing during 1995–2005 but showing a downward trend afterward). In this study, we also deny a strong hydraulic connection between the two lakes. The surface elevations of Selin Co were 4,539 m in 2000 and 4,547.4 m in 2010, which were larger than those of Bange Co (4,522 m from 2000–2010). With such large surface elevation differences of 17 ~ 25 m, a continuously rising Selin Co level was bound to contribute to Bange Co expanding rather than shrinking in recent years. Other studies also attribute dynamic changes in Bange Co and Selin Co to global climatic change and QTP uplift. Based on geomorphologic investigations and optically stimulated luminescence (OSL) dating of paleo-shoreline sediments distributed in northern and eastern Bange Co, Zhao et al. (2018) suggested that the deglacial lake level transgression was likely due to an increase in Northern Hemisphere insolation and corresponding glacial meltwaters, while fluctuations in the lake level during the Holocene were mainly controlled by variations in the Indian summer monsoon. Zhao et al. (2011) pointed out that Bange Co was also influenced by glacier melting, similar to Selin Co. Lv et al. (2003) also attributed dynamic changes in Selin Co and Bange Co to differential rise and fall rates during the time of QTP uplift.

4.2 Limited effect of permafrost degradation on the water budgets of lakes

The effects of permafrost degradation on groundwater discharge and even surface runoff are highly dependent on the permafrost extent of a watershed. Basins with different permafrost extents have contrasting streamflow regime characteristics. Song et al. (2020) proposed more significant effects of permafrost coverage on the annual ratio of the maximum discharge to the minimum discharge (Q_{max}/Q_{min}) for high permafrost cover in QTP subbasins; Q_{max}/Q_{min} ratios was low in the low to moderate (< 50%) permafrost coverage basins, while from the moderate to high (50 ~ 100%) permafrost coverage basins. Ye et al. (2009) described a relationship between the monthly ratio of Q_{max}/Q_{min} and permafrost coverage in the Lena basin and suggested that permafrost conditions strongly affect the discharge regime for regions with high permafrost (> 60%). Although the general applicability of the above statistical relationships exists at larger spatial scales in cross-regional permafrost basins with heterogeneity, a weak positive correlation between lake area increase and permafrost coverage in basins was observed by examining 39 expanding lakes with high permafrost coverage ranging from 65 ~ 99% in an endorheic basin on the QTP (Liu et al. 2020b). The results were mainly attributed to permafrost types, ground ice contents and permafrost thermal conditions. The continuous permafrost coverage in the Selin Co basin was 1.3×10^4 km^2, accounting for 28.6% of the total catchment area. Despite the low

coverage percentage, permafrost in the basin was located on the southern boundary of the continuous permafrost on the QTP, which exhibited more rapid permafrost warming and degradation than that on the central QTP. Additionally, as a consequence of accelerated permafrost degradation, a large amount of ground ice has melted significantly, resulting in profound impacts on lake change.

Similar phenomena also occurred in thermokarst lakes along the Qinghai-Tibet Highway. A field investigation of unmanned aerial vehicles (UAVs) in August 2018, confirmed the existence of abundant thermokarst lakes close to the Qinghai-Tibet railway and highway (Fig. 11). Thermokarst lakes are a typical manifestation of permafrost degradation and develop as a result of the thawing of ice-rich permafrost or the melting of massive ground ice. Thermokarst lakes were spread between the Kunlun Mountain pass and the Fenghuo Mountain pass along the Qinghai-Tibet railway, where ice-rich and warm permafrost exists. The distribution of thermokarst lakes is closely related to the ice content and the permafrost temperature; 83.8% of thermokarst lakes are located in rich-ice permafrost regions, and 54.9% are located in high-temperature permafrost regions (Niu et al. 2011). Permafrost degradation with melting ground ice initially promotes thermokarst, but subsequent lake drainage can further accelerate permafrost degradation (Smith et al. 2005).

The rapid expansion of Selin Co was significantly attributed to the increase in glacier meltwater, followed by that of permafrost meltwater. However, glacier melting and permafrost thawing into lakes should not increase the overall mass of the lakes and may decrease the mass of lakes because a portion of the melted water is lost through evaporation or is discharged to rivers that leave the TP. Additionally, the effect of permafrost degradation on the hydrological regime is complex and involves the potential interactions among climate change, permafrost degradation and groundwater flow; thus, it is difficult to access groundwater discharge to lake recharge. Since it remains challenging to evaluate glacier mass balances and permafrost meltwater, we could not quantify the associated contribution to lake growth.

5 Conclusion

Based on Landsat TM images, ETM + images, OLI images, meteorological data, glacier data and permafrost monitoring data, the dynamic changes in Selin Co and its surrounding small lakes were discussed, and the driving forces behind their changes were further explored. The results suggested that, from 2000 to 2017, the areas of Bange Co and Cuoe Lake showed slow overall increasing trends at rates of 0.28 km^2/yr and 0.11 km^2/yr, respectively, exhibiting upward trends before 2005 but downward trends afterward. The lake level and lake volume of Bange Co slightly rose by 1.64 m and 0.088 km^3, respectively, between 1959 and 2010. The area of Selin Co experienced a rapid expansion of 685.8 km^2 at a rate of 30.39 km^2/yr, displaying a slow increase of 27.11 km^2 from 1988–1997, a rapid increase of 510.53 km^2 from 1997–2005 and an increase of 148.16 km^2 from 2005–2017. The Selin Co level and water volume rapidly rose by 8.138 m and 17.47 km^3, respectively, from 2000–2015. Large changes were observed before 2005; the lake level and water volume significantly increased by 6.92 m and 7.35 km^3, respectively, from 2000–2005. The changes in the areas of Bange Co and Cuoe Lake were consistent with the precipitation trend, and precipitation was the main influencing factor. The dramatic expansion of Selin Co was mainly related to glacial meltwater, followed by accelerated permafrost.

6 Declarations

Conflicts of Interest

The authors declare no conflict of interest.

Acknowledgments

This study was supported by the Natural Science Foundation of Qinghai University (Nos. 2020-QGY-10), the Natural Science Foundation of Qinghai Province, China (Nos. 2021-ZJ-940Q), the Strategic Priority Research Program of Chinese Academy of Sciences (Nos. XDA23060703) and the National Natural Science Foundation of China (No. 41671068). Significant thanks to all author for their contributions; conceptualization and writing (original draft) for Wenhui Liu and Hairui Liu, permafrost data curation for Guangyue Liu and Wu Wang, methodology and software for Qinhao Zhao and Qi Zhang, supervision and grammar editing for Changwei Xie. Thanks to all the staff of the Cryosphere Research Station on the Qinghai-Tibet Plateau, Chinese Academy of Sciences for their hard work in obtaining field permafrost data. Special thanks to Guangyue Liu for providing photo of thermokarst lake.

7 References

1. Bhasang T, Liu JS, Niu JF et al (2012) Area variation and its causes of Bamu Co Lake in the Central Tibet. Journal of Natural Resources 27:128–136. https://doi.org/10.11849/zrzyxb.2012.02.013
2. Bian D, Bianba CR, La B, et al. (2010) The response of water level of Selin Co to climate change during 1975–2008. Acta Geographica Sinica 65: 313–319. https://doi.org/10.11821/xb201003006
3. Cheng GD, Zhao L, Li R et al (2019) Characteristic, changes and impacts of permafrost on Qinghai-Tibet Plateau. Chin Sci Bull 64:278–2795. https://doi.org/10.1360/TB-2019-0191
4. Deji YZ, Nima J, Qiangba OZ, et al. (2018) Lake area variation of Selin Tso in 1975–2016 and its influential factors. Plateau and Mountain Meteorology Research 38: 37–43. https://doi.org/1674-2184(2018) 02-0035-07
5. Du J, Yang TB, He Y (2014) Glaciers and lakes changes and climate response in the Selin Co Basin from 1990 to 2011. Journal of Arid Land Resources and Environment 28: 88–93. https://doi.org/1003-7578(2014) 12-088-06

6. Gui J, Li ZX, Feng Q et al (2019) Characteristics of runoff components in the Gulang River basin of the Qilian Mountains. J Glaciol Geocryol 41: 918–925. https://doi.org/10. 7522/j. issn.1000-0240.2018.1145
7. Hao GB, Wu B, Zhang LF, et al. (2016) Temporal and spatial variation analysis of the area of Siling Co lake in Tibet based on ESTARFM (1976–2014). Journal of Geo-information Science, 18(6):833–846. https://doi.org/10.3724/SP.J.1047.2016.00833
8. Hu GJ, Zhao L, Li R et al (2014) Characteristics of hydro-thermal transfer during freezing and thawing period in permafrost regions. Soils 46(2):355–360. https://doi.org/10.13758/j.cnki.tr.2014.02.026
9. Ji ST (2020) Numerical simulation of permafrost thawing and its impact on changes of lake reserves in Qinghai-Tibet Plateau. Harbin Institute of Technology
10. Kurylyk BL, MacQuarrie KB, McKenzie JM (2014) Climate change impacts on groundwater and soil temperatures in cold and temperate regions:implications, mathematical theory, and emerging simulation tools. Earth Sci Rev 138:313–334. https://doi.org/10.1016/j.earscirev.2014.06.006
11. La B, Chen T, Laba ZM, et al. (2011) Area change of Selincuo Lake and its forming reasons based on MODIS data. Journal of Meteorology and Environment 27: 69–72. https://doi.org/1673- 503X(2011)02-0069-04
12. Lei YB, Yang K, Wang B et al (2014) Response of inland lake dynamics over the Tibetan Plateau to climate change. Clim Chang 125:281–290. https://doi.org/10.1007/s10584-014-1175-3
13. Lei YB, Yao TD, Bird BW et al (2013) Coherent lake growth on the central Tibetan Plateau since the 1970s: Characterization and attribution. J Hydrol 483:61–67. https://doi.org/10.1016/j.jhydrol.2013.01.003
14. Li BY (2000) The last greatest lakes on the Xizang (Tibetan) Plateau. Acta Geogr Sin 55(2):174–182
15. Li JL, Chen X, Bao AM (2011) Spatial-temporal characteristics of lake level changes in central Asia during 2003–2009. Acta Geographica Sinica 66:1219–1229. https://doi.org/10.1111/j.1759-6831.2010.00113.x
16. Li L, Li HM, Shen HY et al (2018) The truth and inter-annual oscillation causes for climate change in the Qinghai-Tibet Plateau. J Glaciol Geocryol 40(6): 1079–1089. https://doi.org/10.7522 /j.issn.1000-0240.2018.0117
17. Li R, Zhao L, Ding YJ, et al. (2012) Temporal and spatial variations of the active layer along the Qinghai-Tibet Highway in a permafrost region. Chin Sci Bul 57: 4609–4616. https://doi:org/10.1007/s11434-012-5323-8
18. Li YK, Liao JG, Guo HD et al (2014) Patterns and potential drivers of dramatic changes in Tibetan lakes, 1972–2010. PLoS One 9:e111890. https://doi:10.1371/journal.pone.0111890
19. Li ZX, Feng Q, Liu W et al (2014) Study on the contribution from cryosphere to runoff in the cold alpine basin: a case study of Hulugou River basin in the Qilian Mountains. Glob Planet Chang 122:345–361. http://dx.doi.org/10.1016/j.gloplacha.2014.10.001
20. Li ZX, Feng Q, Wang QJ et al (2016) Contribution from frozen soil meltwater to runoff in an in-land river basin under water scarcity by isotopic tracing in northwestern China. Glob Planet Chang 136:41–51. http://dx.doi.org/10.1016/j.gloplacha.2015.12.002
21. Liao C, Zhuang QL (2017) Quantifying the role of permafrost distribution in groundwater and surface water interactions using a three-dimensional hydrological model. Arct Antarct Alp Res 49:81–100. https://doi.org/10.1657/AAAR0016-022
22. Liao JJ, Shen GZ, Zhao Y (2018) The globe lake level change dataset based on ENVISAT/RA-2, Cryosat-2/SIRAL, Jason-2 radar altimetry data (2002–2016). Global Change Scientific Research Data Publishing System. https://doi.org/10.3974/geodb.2018.05.12.V1
23. Liu GY, Zhao L, Xie CW et al (2016) Variation characteristics and impact factors of the depth of zero annual amplitude of ground temperature in permafrost regions on the Tibetan Plateau. J Glaciol Geocryol 38:1189–1200. https://doi.org/10.7522 /j.issn.1000-0240.2016. 0139
24. Liu JS, Wang SY, Yu SM et al (2009) Climate warming and growth of high-elevation inland lakes on the Tibetan Plateau. Glob Planet Chang 67:209–217. https://doi.org/10.1016/j.gloplacha.2009.03.010
25. Liu L, Jiang LM, Xiang LW et al (2019) The effect of glacier melting on lake volume change in the Siling Co basin (5Z2), Tibetan Plateau. Chinese J Geophys 62:1603–1612. https://doi.org/10.6038/cjg2019M0273
26. Liu WH, Xie CW, Wang W et al (2020b) The impact of permafrost degradation on lake changes in the endorheic basin on the Qinghai-Tibet Plateau. Water 12:1287. https://doi.org/10.3390/w12051287
27. Liu WH, Xie CW, Zhao L et al (2019) Dynamic changes in lakes in the Hoh Xil region before and after the 2011 outburst of Zonag Lake. J Mt Sci 16:1098–1110. https://doi.org/10.1007/s11629-018-5085-0
28. Liu WH, Xie CW, Zhao L et al (2020a) Rapid expansion of lakes in the endorheic basin on the Qinghai-Tibet Plateau since 2000 and its potential drivers. Catena 197. https://doi.org/10.1016/j.catena.2020.104942
29. Lv P, Qu YG, Li QB et al (2003) Selin Co and Bange Co extensional lake basins in the northern part of Tibet and present chasmic activities. Jilin Geology (2):15–19
30. Ma RH, Yang GS, Duan HT et al (2011) China's lakes at present: Number, area and spatial distribution. Sci China Earth Sci 54: 283–289. https://doi.org/10.1007/s11430-010-4052-6
31. Meng K, Shi XH, Wang EQ et al (2012a) High-altitude salt lake elevation changes and glacial ablation in Central Tibet, 2000–2010. Chin Sci Bul 57: 525–534. https://doi.org/doi: 10.1007/s11434-011-4849-5
32. Meng K, Shi XH, Wang EQ et al (2012b) Geomorphic characteristics, spatial distribution of paleoshrelines around the Siling Co area, central Tibetan Plateau, and the lake evolution within the plateau. Chinese Journal of Geology 47:730–745
33. Niu FJ, Lin ZJ, Liu H et al (2011) Characteristics of thermokarst lakes and their influence on permafrost in Qinghai-Tibet Plateau. Geomorphology 132(3–4):222–233. https://doi.org/10.1016/j.geomorph.2011.05.011

34. Niu L, Ye BS, Li J et al (2011) Effect of permafrost degradation on hydrological processes in typical basins with various permafrost coverage in Western China. Sci China Earth Sci 54:615–624. https://doi.org/10.1007/s11430-010-4073-1
35. Pang QQ, Zhao L, Li SX et al (2011) Active layer thickness variations on the Qinghai-Tibet Plateau under the scenarios of climate change. Environ Earth Sci 66(3):849–857. https://doi.org/10.1007/s12665-011-1296-1
36. Qin YH, Wu TH, Zhao L et al (2017) Numerical modeling of the active layer thickness and permafrost thermal state across Qinghai-Tibetan Plateau. J Geophys Res-Atmos 122:11604–11620. https://doi.org/10.1002/2017JD026858
37. Shi YF, Liu XD, Li BY et al (1999) A very strong summer monsoon event during 30–40 ka BP in the Qinghai-Xizang (Tibet) Plateau and its relation to precessional cycle. Chin Sci Bul 44:1851–1858. https://doi.org/10.1007/BF02886339
38. Shi YF, Yu G, Liu XD et al (2001) Reconstruction of the 30–40 ka BP enhanced Indian monsoon climate based on geological records from the Tibetan Plateau. Palaeogeogr Palaeocl Palaeoec 169:69–83. https://doi.org/10.1016/S0031-0182(01)00216-4
39. Song CL, Wang GX, Mao TX et al (2020) Linkage between permafrost distribution and river runoff changes across the Arctic and the Tibetan Plateau. Sci China Earth Sci 63:128–138. https://doi.org/10.1007/s11430-018-9383-6
40. Song CQ, Huang B, Ke LH (2013) Modeling and analysis of lake water storage changes on the Tibetan Plateau using multi-mission satellite data. Remote Sens Environ 135:25–35. http://dx.doi.org/10.1016/j.rse.2013.03.013
41. Song CQ, Huang B, Richards K et al (2014) Accelerated lake expansion on the Tibetan Plateau in the 2000s: Induced by glacial melting or other processes? Water Resour Res 50:3170–3186. https://doi.org/10.1002/2013WR014724
42. Sun Z, Zhao L, Hu GJ et al (2020) Modeling permafrost changes on the Qinghai-Tibetan Plateau from 1966 to 2100: A case study from two boreholes along the Qinghai-Tibet engineering corridor. Permafr Periglac Process 31:156–171. https://doi.org/10.1002/ppp.2022
43. Walvoord MA, Kurylyk BL (2016) Hydrologic impacts of thawing permafrost-a review. Vadose Zone J 15:1–20. https://doi.org/10.2136/vzj2016.01.0010
44. Walvoord MA, Voss CI, Wellman TP (2012) Influence of permafrost distribution on groundwater flow in the context of climate-driven permafrost thaw: example from Yukon Flats Basin, Alaska, United States. Water Resour Res 48:W07524. https://doi.org/10.1029/2011WR011595
45. Wang GX, Hu HC, Li TB (2009) The influence of freeze-thaw cycles of active soil layer on surface runoff in a permafrost watershed. J Hydrol 375:438–449. http://dx.doi.org/10.1016/j.jhydrol.2009.06.046
46. Wang QX, Chen RS, Han CT et al (2018) Changes in river discharge in typical mountain permafrost catchments, northwestern China. Quat Int. https://doi.org/10.1016/j.quaint.2018.11.010
47. Wang QX, Chen RS, Yang Y (2017) Effects of permafrost degradation on the hydrological regime in the source regions of the Yangtze and Yellow rivers, China. Water 9:897. http://dx.doi.org/doi:10.3390/w9110897
48. Woo MK, Kane DL, Carey SK et al (2008) Progress in permafrost hydrology in the New Millennium. Permafr Periglac Process 19:237–254. https://doi.org/10.1002/ppp.613
49. Wu JC, Sheng Y, Wu QB et al (2009) Discussion on the possibility of taking ground ice in permafrost regions as water sources under climate warming. J Glaciol Geocryol 31:351–356. https://doi.org/1000-0240(2009)02-0350-07
50. Wu QB, Zhang TJ (2010) Changes in active layer thickness over the Qinghai-Tibetan Plateau from 1995 to 2007. J Geophys Res 115:1–12. https://doi.org/10.1029/2009JD012974
51. Wu QB, Zhang TJ, Liu YZ (2010) Permafrost temperatures and thickness on the Qinghai-Tibet Plateau. Glob Planet Chang 72: 32–38. https://doi.org/10.1016/j.gloplacha.2010.03.001
52. Xie CW, William AG, Zhao L et al (2015) Temperature-dependent adjustments of the permafrost thermal profiles on the Qinghai-Tibet Plateau, China. Arct Antarct Alp Res 47:719–728. http://dx.doi.org/10.1657/AAAR00C-13-128
53. Xie CW, Zhao L, Wu TH, et al. (2012) Changes in the thermal and hydraulic regime within the active layer in the Qinghai-Tibet Plateau. J Mt Sci 9: 483–491. https://doi:org10.1007/s11629-012-2352-3
54. Yang DQ, Robinson D, Zhao YY et al (2003) Streamflow response to seasonal snow cover extent changes in large Siberian watersheds. J Geophys Res 108(D18):4578. https://doi.org/10.1029/2002JD003149
55. Yang K, Ye BS, Zhou DG et al (2011) Response of hydrological cycle to recent climate changes in the Tibetan Plateau. Clim Chang 109:517–534. https://doi.org/10.1007/s10584-011-0099-4
56. Yang KH, Yao FF, Wang JD et al (2017A) Recent dynamics of alpine lakes on the endorheic Changtang Plateau from multi-mission satellite data. J Hydrol 552:633–645. https://doi.org/10.1016/j.jhydrol.2017.07.024
57. Yang RM, Zhu LP, Wang JB et al (2017B) Spatiotemporal variations in volume of closed lakes on the Tibetan Plateau and their climatic responses from 1976 to 2013. Clim Chang 140:621–633. https://doi.org/10.1007/s10584-016-1877-9
58. Yao FF, Wang JD, Yang KH et al (2018) Lake storage variation on the endorheic Tibetan Plateau and its attribution to climate change since the new millennium. Environ Res Lett 13:064011. https://doi.org/10.1088/1748-9326/aab5d3
59. Ye QH, Zong JB, Tian LD et al (2017) Glacier changes on the Tibetan Plateau derived from Landsat imagery: mid-1970s-2000-2013. J Glaciol Geocryol 63:273–287. https://doi.org/10.1017/jog.2016.137
60. Zhang GQ, Bolch T, Chen WF et al (2021) Comprehensive estimation of lake volume changes on the Tibetan Plateau during197-2019 and basin-wide glacier contribution. Sci Total Environ. https://doi.org/10.1016/j.scitotenv.2021.145463

61. Zhang GQ, Li JL, Zheng GX et al (2017c) Lake-area mapping in the Tibetan Plateau: an evaluation of data and methods. Int J Remote Sens 38:742–772. http://dx.doi.org/10.1080/01431161.2016.1271478
62. Zhang GQ, Xie HJ, Yao TD et al (2013) Water balance estimates of ten greatest lakes in China using ICESat and Landsat data. Chin Sci Bull 58:38153829. https://doi.org/10.1007/ s11434-013-5818-y
63. Zhang GQ, Yao TD, Chen WF et al (2018) Regional differences of lake evolution across China during 1960s–2015 and its natural and anthropogenic causes. Remote Sens Environ 221:386–404. doi 10.1016/j.rse.2018.11.038
64. Zhang GQ, Yao TD, Piao SL et al (2017a) Extensive and drastically different alpine lake changes on Asia's high plateaus during the past four decades. Geophys Res Lett 44:252–260. https://doi.org/10.1002/2016GL072033
65. Zhang GQ, Yao TD, Shum CK et al (2017b) Lake volume and groundwater storage variations in Tibetan Plateaus endorheic basin. Geophys Res Lett 44:5550–5560. https://doi.org/10.1002/2017GL073773
66. Zhang GQ, Yao TD, Xie HJ et al (2014) Lakes' state and abundance across the Tibetan Plateau. Chin Sci Bul 59:3010–3021. https://doi.org/10.1007/s11434-014-0258-x
67. Zhang YS, Yao TD, Ma YZ. (2011) Climatic changes have led to significant expansion of endorheic lakes in Xizang (Tibet) since 1995. Sciences in Cold and Arid Regions 3: 0463–0467. https://doi.org/10.3724/SP.J.1226.2011.00463
68. Zhang YS, Yao TD, Pu JC et al (1997) The features of hydrological processes in the Dongkemadi River Basin, Tanggula Pass, Tibetan Plateau. J Glaciol Geocryol 019(003):214–222
69. Zhao GT, Du YS, Wei HC et al (2018) Optically stimulated luminescence dating of Paleo-shorelines of Bange Co, Qinghai-Tibetan Plateau and its implications for Palaeo-environment. Journal of Salt Research 26(3):26–34
70. Zhao L, Cheng GD, Li SX et al (2000) Thawing and freezing processes of active layer in Wudaoliang region of Tibetan Plateau. Chin Sci Bul 45(23):2181–2187. https://doi.org/10.1007/BF02886326
71. Zhao L, Zou DF, Hu GJ et al (2020) Changing climate and the permafrost environment on the Qinghai-Tibet (Xizang) Plateau. Permafr Periglac Process 1–10. https://doi.org/10.1002/ppp.2056
72. Zhao XT, Wu ZH, Hu DG et al (2005) The discovery of late Pleistocene highstand lacustrine sediments of the Co Ngoin Lake and adjacent areas, Tibet. Acta Geoscientica Sinica 26(4):291–298
73. Zhao XT, Zhao YY, Zheng MP et al (2011) Late Quaternary lake development and denivellation of Bankog Co as well as lake evolution of Southeastern North Tibetan Plateau during the last great lake period. Acta Geoscientica Sinica 32(1):13–26
74. Zhao XT, Zhu DG, Wu ZH et al (2002) The development of Nam Co Lake in Tibet since Lake Pleistocene. Acta Geoscientica Sinica 23(4):329–334
75. Zhao YY, Zheng MP, Cai XG et al (2004) Modern lake resources and environment on the western side of the Tibet section of the phase-II project of the Qinghai-Tibet Railway. Geological Bulletin of China (7): 680–685
76. Zhao YY, Zhao XT, Zheng MP et al (2006) The denivellation of Bankog Co in the past 50 years, Tibet. Acta Geol Sin 80:876–884
77. Zheng MP, Yuan HR, Zhao XT et al (2000) The Quaternary Pan-lake(overflow) period and paleoclimate on the Qinghai Tibet Plateau. Acta Geological Sinica 80(2):169–180
78. Zhou J, Wang L, Zhang YS et al (2016) Spatiotemporal variations of actual evapotranspiration over the Lake Selin Co and surrounding small lakes (Tibetan Plateau) during 2003–2012. Sci China Earth Sci 59(12):2441–2453. https://doi.org/10.1007/s11430-016-0023-6
79. Zhou J, Wang L, Zhang YS, et al. (2015) Exploring the water storage changes in the largest lake (Selin Co) over the Tibetan Plateau during 2003–2012 from a basin-wide hydrological modeling. Water Resour Res 51: 8060–8086. https://doi.org/10.1002/2014WR015846
80. Zhu DG, Meng XG, Zhao XT et al (2001) Nam Tso lacustrine sediments and the ancient big lake in northern Tibet Plateau. Acta Geoscientica Sinica 22(2):149–155
81. Zhu DG, Zhao XT, Meng XG et al (2003) Lake level fluctuation of Nam Co, Tibet, since the late Pleistocene, and evolution of an ancient large lake on the northern Tibetan Plateau. Geological Bulletin of China 22(11):918–927
82. Zou DF, Zhao L, Sheng Y et al (2017) A new map of the permafrost distribution on the Tibetan Plateau. Cryosphere 11:2527–2542. https://doi.org/10.5194/tc-11-2527-2017

Figures

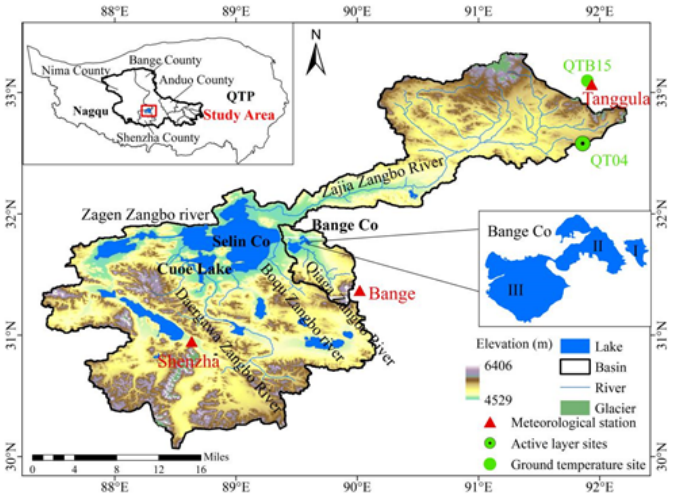

Figure 1

A schematic representation of the study area. The digital elevation model was obtained from ASTER GDEM version 2.0 (http://www.gscloud.cn); the drainage basins were extracted from the HydroSHEDS dataset (http://hydrosheds.cr.usgs.gov); the glacier data shown were obtained from the First Glacier Inventory of China (images during 1950-1980); and the lake areas shown were from 2017. Note: The designations employed and the presentation of the material on this map do not imply the expression of any opinion whatsoever on the part of Research Square concerning the legal status of any country, territory, city or area or of its authorities, or concerning the delimitation of its frontiers or boundaries. This map has been provided by the authors.

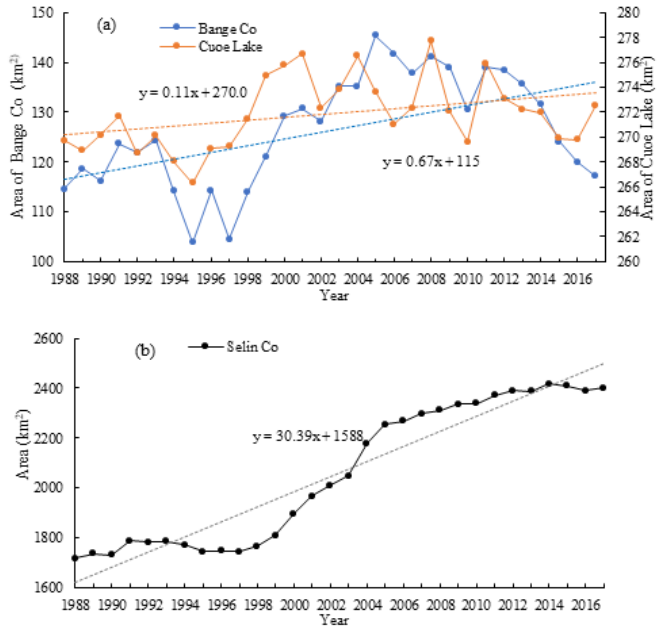

Figure 2

Annual changes in the areas of Bange Co, Cuoe Lake and Selin Co from 1988-2017.

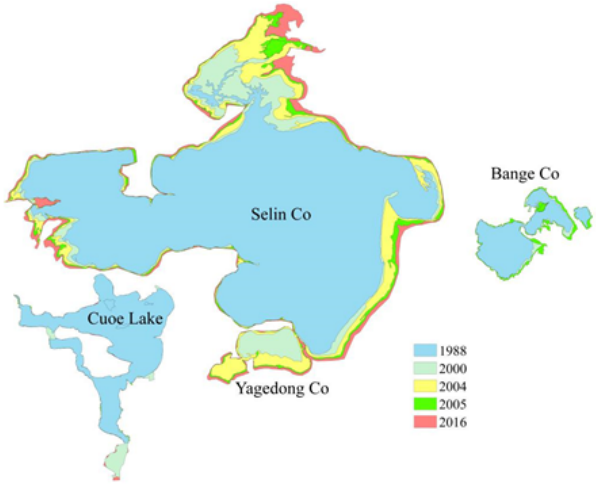

Figure 3

Changes in the shapes of Bange Co, Cuoe Lake and Selin Co. Note: The designations employed and the presentation of the material on this map do not imply the expression of any opinion whatsoever on the part of Research Square concerning the legal status of any country, territory, city or area or of its authorities, or concerning the delimitation of its frontiers or boundaries. This map has been provided by the authors.

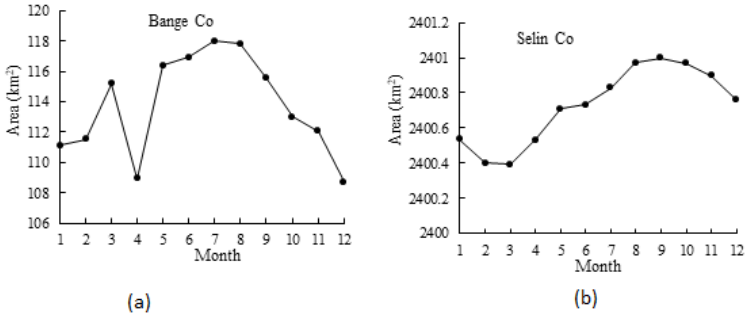

Figure 4

Seasonal changes in the averaged area of (a) Bange Co and (b) Selin Co during the period from 2015 to 2017.

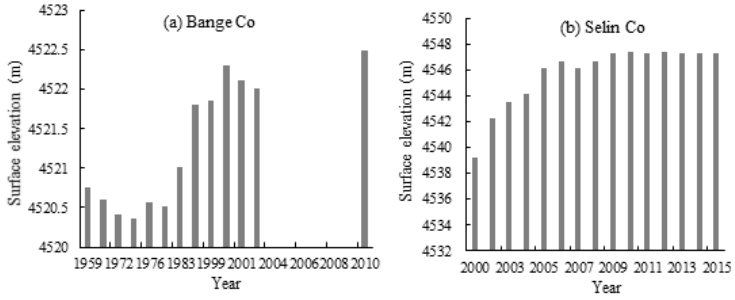

Figure 5

Changes in the surface elevations of Bange Co and Selin Co.

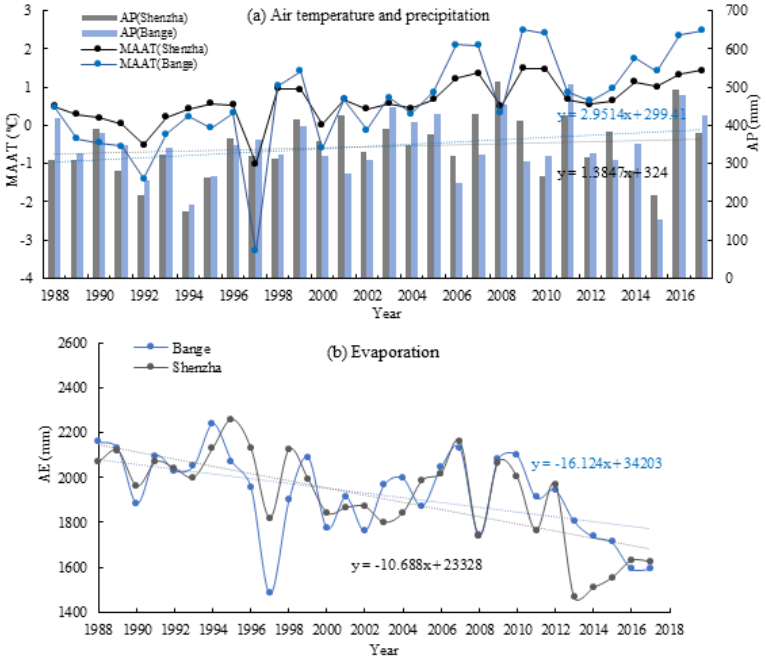

Figure 6

The annual precipitation and mean annual air temperature at the Shenzha and Bange meteorological stations from 1988 to 2017.

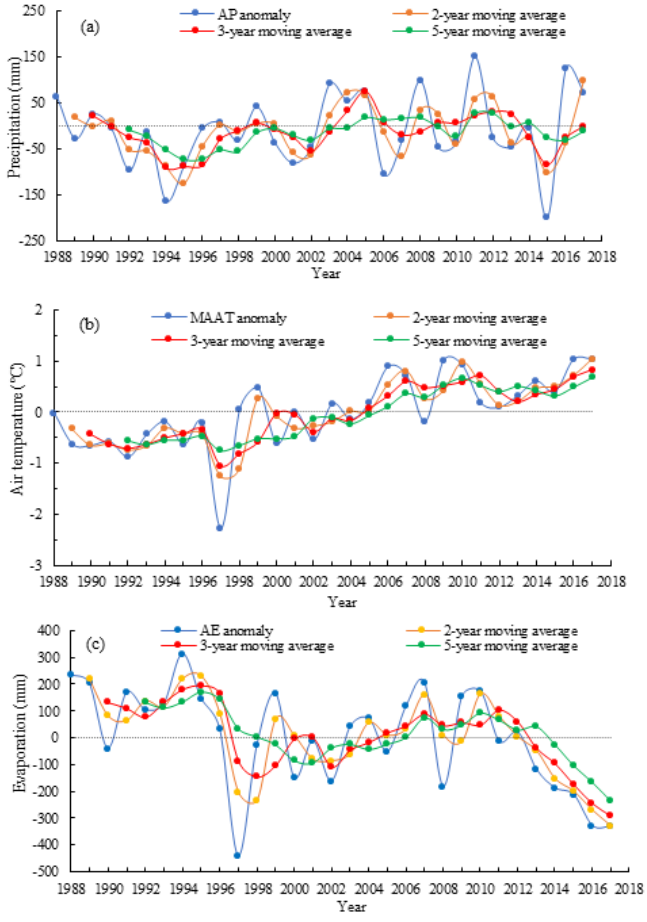

Figure 7

The annual anomaly changes in the AP, MAAT and AE at the Bange meteorological station from 1988 to 2017.

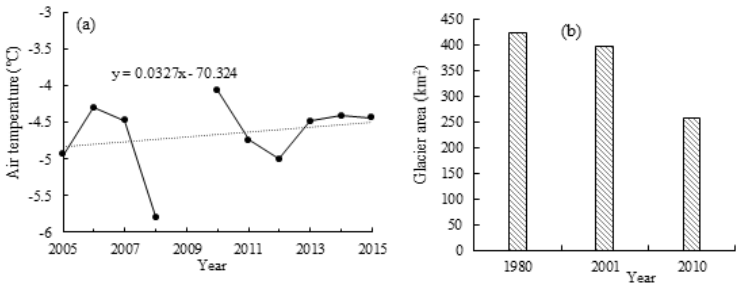

Figure 8

a) The MAAT at the Tanggula meteorological station recorded from 2005 to 2015; (b) the change in total glacier area for different periods in the Selin Co basin (the glacier areas shown in 1980 and 2010 were extracted from the First Glacier Inventory of China (images taken from 1950-1980) and the Second Glacier Inventory of China (images taken from 2006-2010)). The glacier areas in 2001 (images taken from 1999-2002) produced by Ye et al. (2017) are shown.

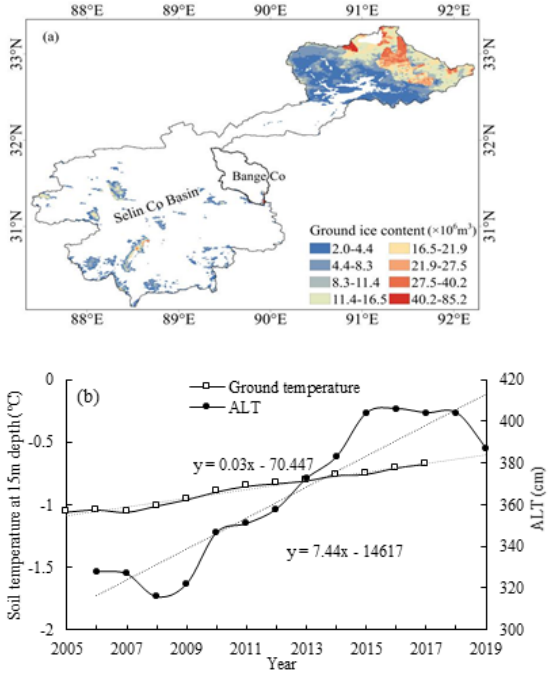

Figure 9

(a) The distribution of ground ice content over the Selin Co and Bange Co catchments; (b) the annual changes in the ALT at the QT04 observation site and in the soil temperature at a 15-m permafrost depth recorded at the QTB15 observation site. Note: The designations employed and the presentation of the material on this map do not imply the expression of any opinion whatsoever on the part of Research Square concerning the legal status of any country, territory, city or area or of its authorities, or concerning the delimitation of its frontiers or boundaries. This map has been provided by the authors.

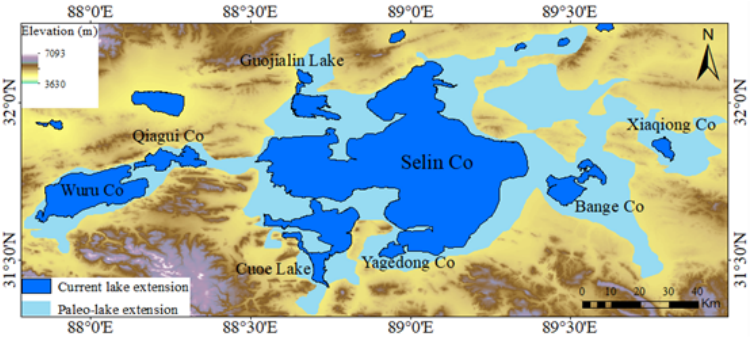

Figure 10

The linkage between Selin Co and the surrounding lakes. The gray-blue area shows the paleo-Selin Co extension delineated by the altitudes of the highstand shorelines; the blue area indicates the current levels of the lakes around Selin Co (modified from Meng et al. 2012b). Note: The designations employed and

the presentation of the material on this map do not imply the expression of any opinion whatsoever on the part of Research Square concerning the legal status of any country, territory, city or area or of its authorities, or concerning the delimitation of its frontiers or boundaries. This map has been provided by the authors.

Figure 11

Thermokarst lakes discovered by a UAV survey along the Qinghai-Tibet railway and highway in September 2019.